

Electronic Supplementary Information

Photoluminescence Enhancement and High Accuracy Patterning of Lead Halide Perovskite Single Crystals by MeV Ion Beam Irradiation

Milan Palei^{a,∇,+}, M Motapothula^{b,Ⓛ,+}, Aniruddha Ray^{a,c}, Ahmed L. Abdelhady^a, Luca Lanzano^d, Mirko Prato^e, Jaya K. Panda^f, Alice Scarpellini^g, Vittorio Pellegrini^f, Daniel Primetzhofer^b, Urko Petralanda^{a,Σ,*}, Liberato Manna^{a,*}, Zhiya Dang^{a,Ⓛ,*}

a, Department of Nanochemistry, Istituto Italiano di Tecnologia, Via Morego 30, Genova, Italy, 16163

b, Department of Physics and Astronomy, Uppsala University, Box 516, S-751 20 Uppsala, Sweden

c, Dipartimento di Chimica e Chimica Industriale, Università degli Studi di Genova, Via Dodecaneso 31, 16146 Genova, Italy

d, Nanoscopy and NIC, Istituto Italiano di Tecnologia, Via Enrico Melen 83, Building B, Genova, Italy, 16152

e, Materials Characterization Facility, Istituto Italiano di Tecnologia, Via Morego 30, Genova, Italy, 16163

f, Graphene Labs, Istituto Italiano di Tecnologia, Via Morego 30, Genova, Italy, 16163

g, Electron Microscopy Facility, Istituto Italiano di Tecnologia, Via Morego 30, Genova, Italy, 16163

Corresponding Author

* upeho@dtu.dk, liberato.manna@iit.it, dangzhy3@mail.sysu.edu.cn

1. Experimental Methods

Growth of MAPbBr₃ single crystals

Typically, 1M solution of MABr and PbBr₂ was prepared in DMF. The solution was then filtered using PTFE filter with 0.2-mm pore size and the filtrate was placed in a vial that was placed in a heating block at 60 °C. Next, the temperature was increased gradually to 80 °C and the vial was left undisturbed for 3 hours. The obtained crystals were dried in a vacuum oven at 40 °C overnight then the crystals were stored in the glovebox until needed.

Absorbance measurements

Steady-state absorbance measurement of the MAPbBr₃ single crystal was carried out in transmission mode using a Cary 5000 spectrophotometer equipped with an integrating sphere.

XRD measurements

X-ray Diffraction analysis was performed using Panalytical Empyrean X-ray diffractometer equipped with a 1.8 kW Cu K α ceramic X-ray tube and a PIXcel3D 2 × 2 area detector, operating at 45 kV and 40 mA. The single crystal was studied under ambient conditions using the parallel beam bragg Brentano geometry. XRD data was collected with a step size of 0.013° and a scan speed of 0.013°/s and the analyses was carried out using the HighScore 4.1 software from PANalytical.

X-ray Photoelectron Spectroscopy (XPS)

A Kratos Axis Ultra DLD spectrometer equipped with a monochromatic Al K α source (photon energy = 1486.6 eV) was used for XPS characterization. Relative atomic percentages of different species were computed from high-resolution spectra, fitted with Voigt functions using CasaXPS software.

Photoluminescence imaging

The spectrally resolved images were recorded with an emission detection bandwidth of 2.5 nm over a spectral wavelength of 498-578 nm. We used 10 \times and 20 \times air (Nikon CFI Plan Apo Lambda 10 \times 0.45 NA) objective lens. The spectral profiles of ion beam exposed and un-exposed area were obtained by drawing rectangular regions of interest around.

FLIM measurements

Photoluminescence was excited at 488 nm with a laser diode modulated at 10 MHz. The PL signal was detected in the spectral emission range 500-550nm. The frame size was set to 512 \times 512 pixels and the scanning pixel-dwell time was set at 12.1 μ s/pixel. Each FLIM image was obtained by averaging over 20 frames corresponding to an acquisition time of \sim 1 min. The FLIM data acquisition was managed by the VistaVision software (ISS). For each pixel, the FLIM system recorded a value of phase delay (ϕ) and de-modulation (M) at multiple frequencies with respect to the excitation signal. The FLIM data were visualized in the phasor plot where $g=M \cos(\phi)$ and $s=M \sin(\phi)$.¹ Before the experiments, the system was calibrated with a solution of Fluorescein in 1M NaOH, which has a known single exponential lifetime of 4.1 ns. In a typical FD FLIM measurement a sinusoidally modulated source excites the sample and the outcoming emission signal is still a sine wave, but has undergone modulation and phase shift with respect to the source. The modulation ratio (M) and phase change (ϕ) are derived from Phasor plot and their corresponding lifetime contributions (modulation lifetime (τ_M) and phase lifetime (τ_ϕ)) are given by²

$$\tau_M = \frac{1}{\omega} \left(\frac{1}{M^2} - 1 \right)^{\frac{1}{2}} \quad (1)$$

$$\tau_\phi = \left(\frac{1}{\omega} \right) \tan\phi \quad (2)$$

TCSPC measurement

TCSPC measurements were performed for bulk pristine sample without any irradiation using Edinburgh instrument fluorescence spectrometer (FLS 920). The PL decay traces were recorded by exciting the sample at 405 nm with a pulsed diode laser with a 50 ps at a repetition rate of 0.05-1 MHz.

ToF- ERDA Measurement

In order to quantify the low Z elements of MAPbBr₃ single crystals, Time of flight elastic recoil detection analysis (ToF-ERDA) measurements were carried out. 36 MeV iodine beam was collimated using a circular aperture in the beamline and focused to a spot size of \sim 1 mm on the sample surface, while the sample was tilted 62.5 degrees w.r.t beam direction and the recoiled elements were captured by a ToF detector which is kept 13.75 degrees in the direction of the incident beam. Since the sample was tilted w.r.t the incident beam direction the beam shape turns into an elliptic.

2. Ion penetration depth

Table S1. The penetration depths of used ions in MAPbBr₃ and Cu

	3MeV He ⁺	12.5MeV Br ⁵⁺	20MeV I ⁷⁺
Cu (μm)	5.49	2.43	2.91
MAPbBr ₃ (μm)	24.7	11.4	14.3

3. PL maps and spectra peak analysis

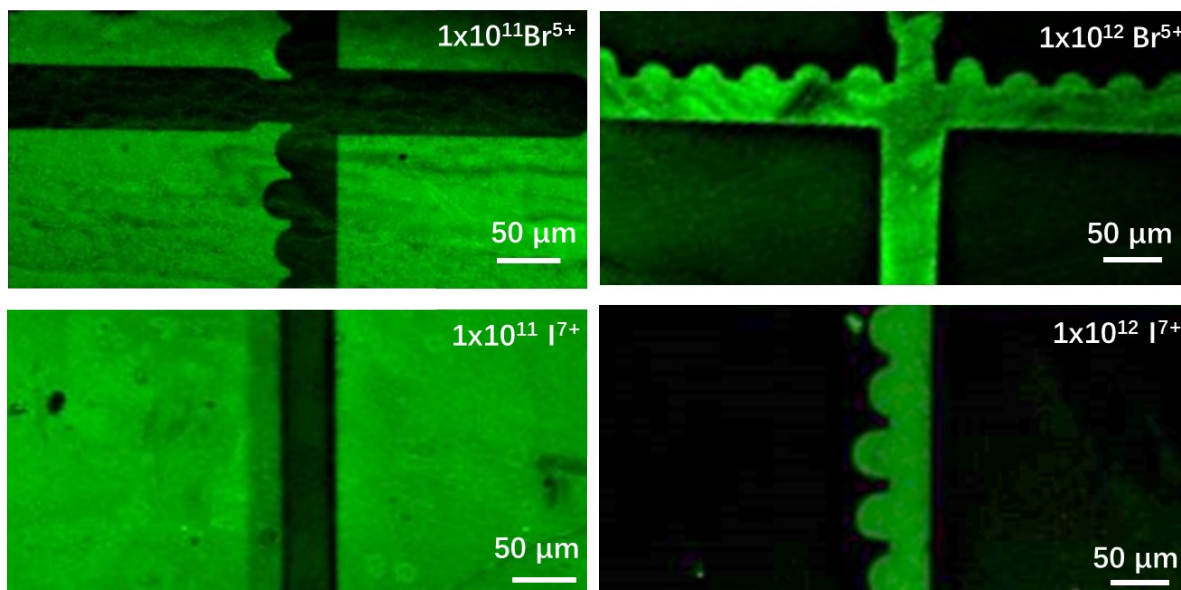


Fig. S1.1 PL confocal maps for patterned MAPbBr₃ crystal surfaces.

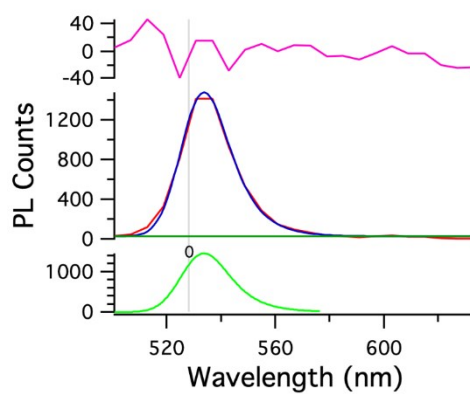


Fig. S1.2 PL spectra (red) obtained from masked (unexposed) MAPbBr₃ crystal and its fitting with expmodGauss function; where blue = fitted curve, green = peak1 and pink = residue after curve fitting.

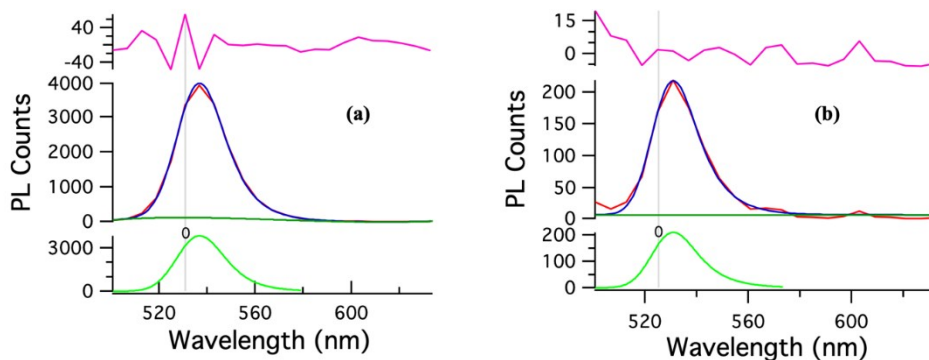


Fig. S1.3 PL spectra obtained from the ion exposed surface (a) low dose area (1×10^{11} I/cm²) (b) high dose area (1×10^{12} I/cm²) of 12.5MeV I⁷⁺ and are fitted with expmodGauss function; where blue = fitted curve, green = peak1 and pink = residue after curve fitting

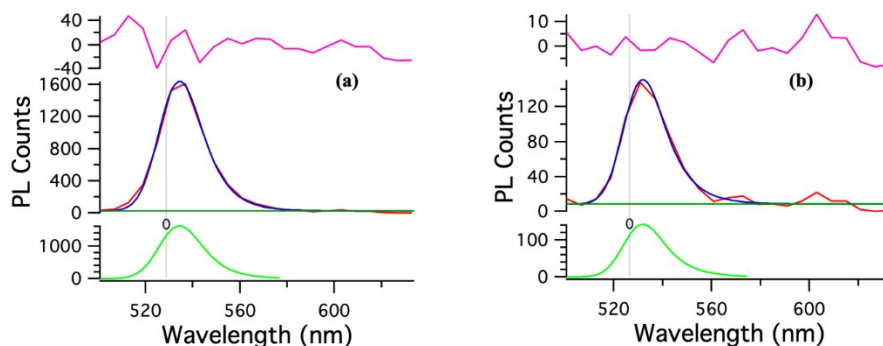


Fig. S1.4 PL spectra obtained from the ion exposed surface (a) low dose area (1×10^{11} Br/cm²) (b) high dose area (1×10^{12} Br/cm²) of 12.5MeV Br⁵⁺ and are fitted with expmodGauss function; where blue = fitted curve, green = peak1 and pink = residue after curve fitting

Table S2. The peak position and FWHM of PL peaks for patterned surfaces (both pristine crystal and areas irradiated with ion beam), obtained from fitting of all spectra with Voigt function, and background with log-polynomial function

Ion irradiation conditions	Peak position (nm)	FWHM (nm)
No exposure	533.7	21.547
1×10^{11} I/cm ²	535.14	20.318
1×10^{12} I/cm ²	530.94	21.188
1×10^{11} Br/cm ²	534.37	22.158
1×10^{12} Br/cm ²	531.91	20.587

4. Fluorescence lifetime imaging and time correlated single photon counting measurement

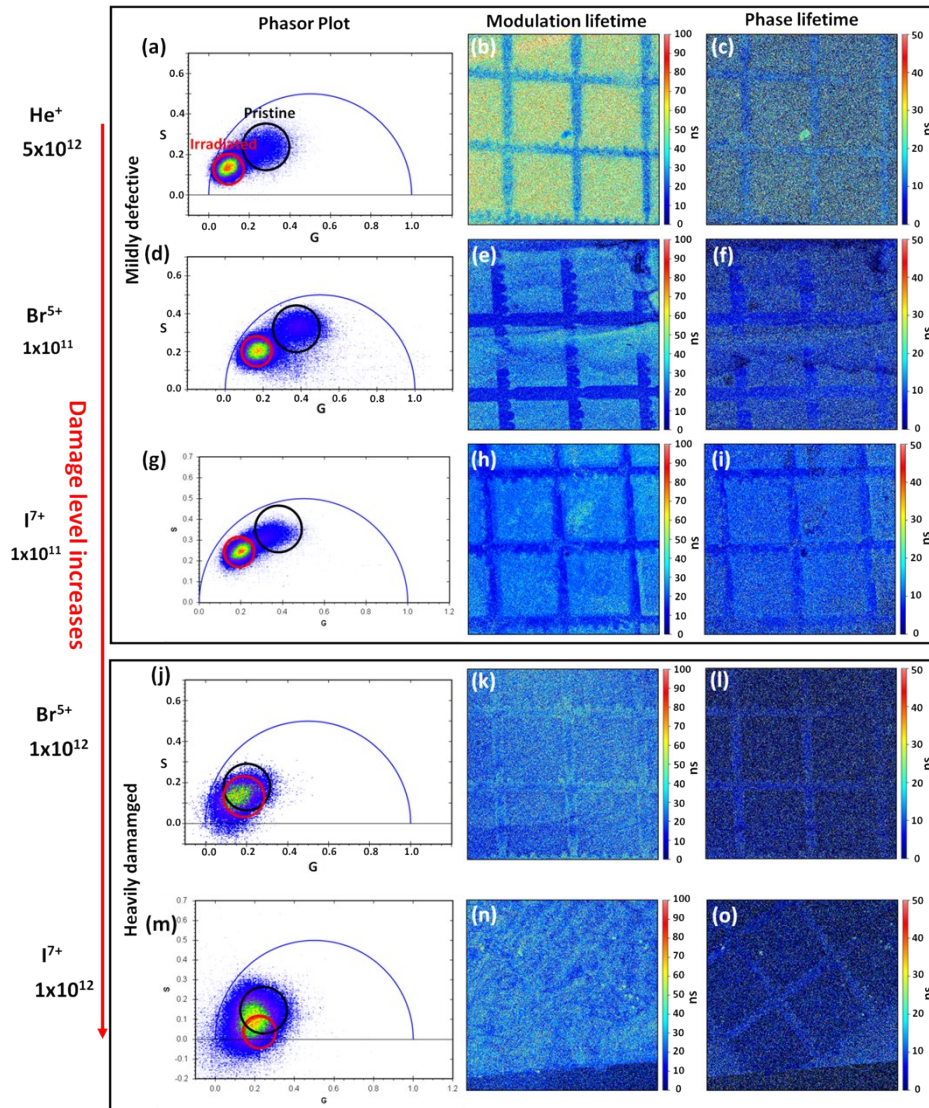


Fig. S2.1 FLIM imaging: Phasor plot, modulation lifetime map, phase lifetime map of samples patterned with six different conditions in the order that surface defect density increases from top row to bottom row.

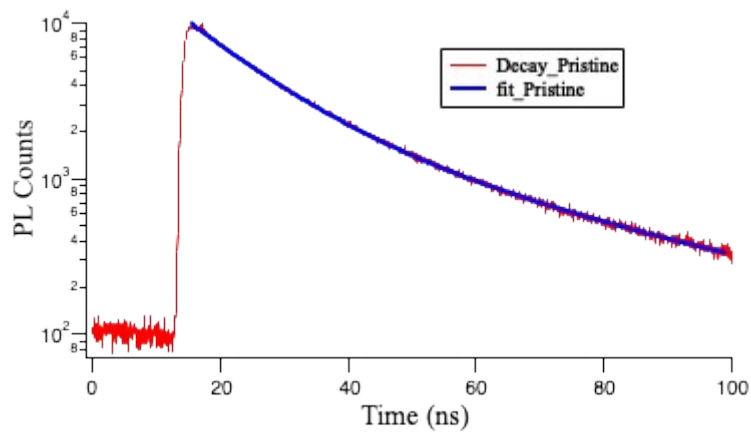


Fig. S2.2 TCSPC decay curve measured on a pristine MAPbBr₃ single crystal and its fitted plot.

5. Electron beam energy loss along the depth in MAPbBr₃

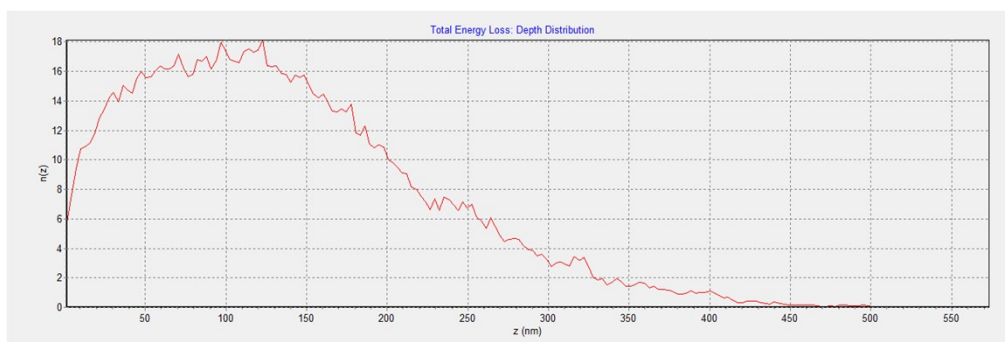


Fig. S3 The calculated depth distribution of energy loss for 5kV electrons incident on MAPbBr₃

6. Composition analysis of heavily damaged MAPbBr₃

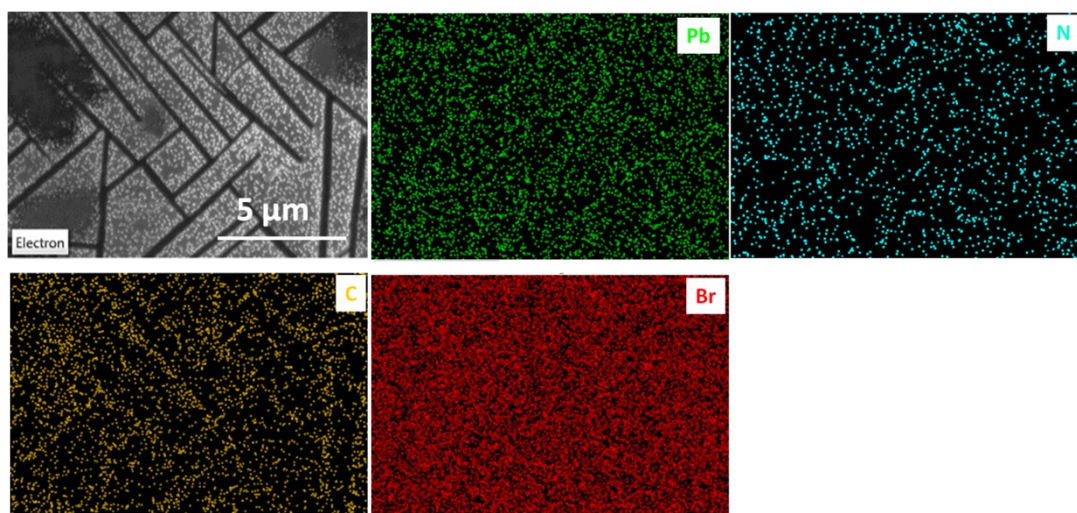


Fig. S4.1 SEM image of an irradiated region on heavily damaged crystal by high dose Br⁵⁺, and corresponding elemental maps of C, N, Pb, Br by EDS.

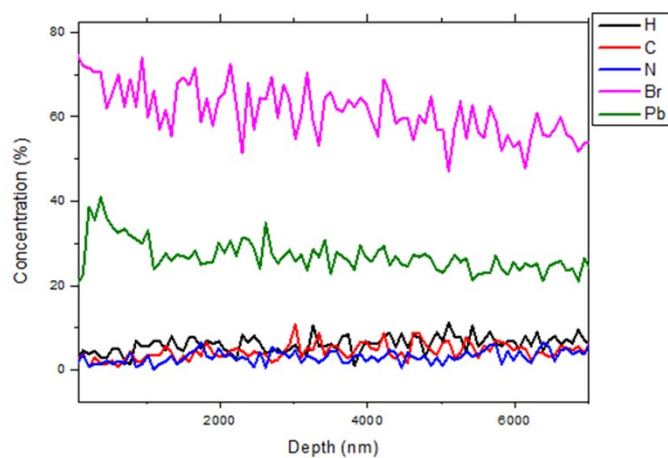


Fig. S4.2 ERDA measurements of the elemental distribution along the depth with accumulated dose equal to heavily damaged crystal by high dose I⁷⁺.

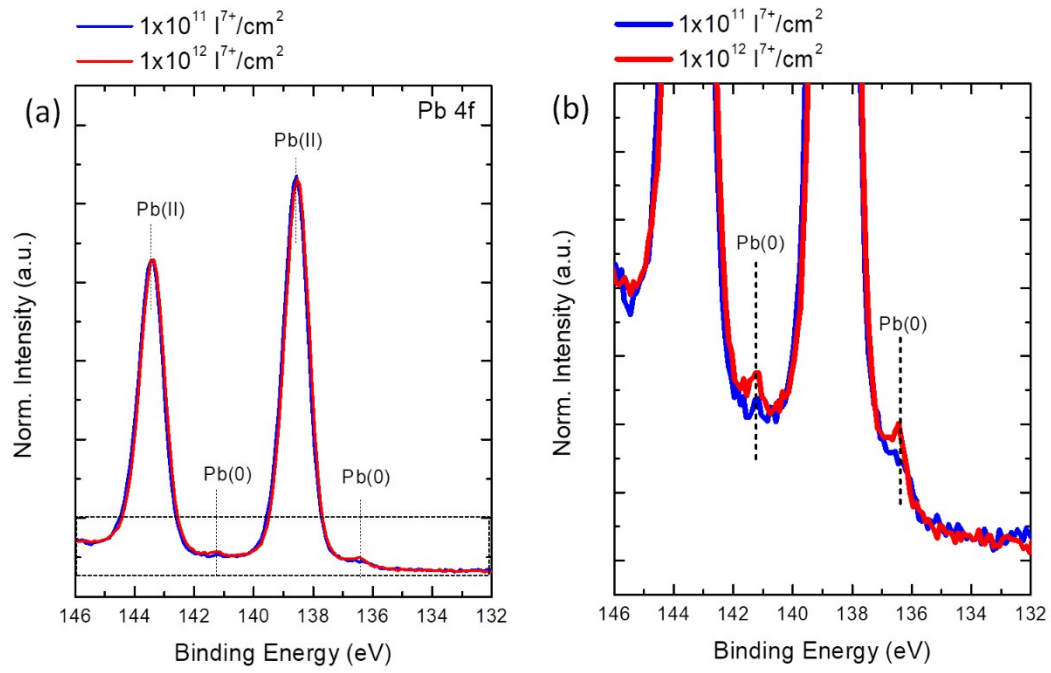


Fig. S4.3 (a) XPS spectra of the crystal surfaces patterned by $1 \times 10^{11} \text{ I}^{7+}/\text{cm}^2$ and $1 \times 10^{12} \text{ I}^{7+}/\text{cm}^2$; (b) zoomed in of the spectra within the black dashed square of panel (a). Quantification results show that the Pb^0 is approx. 0.8% of the whole Pb content on the surface patterned by $1 \times 10^{11} \text{ I}^{7+}/\text{cm}^2$, and instead it is approx. 1.7% of the total Pb content for $1 \times 10^{12} \text{ I}^{7+}/\text{cm}^2$.

7. A calculation of the surface Frenkel defect density based on SRIM

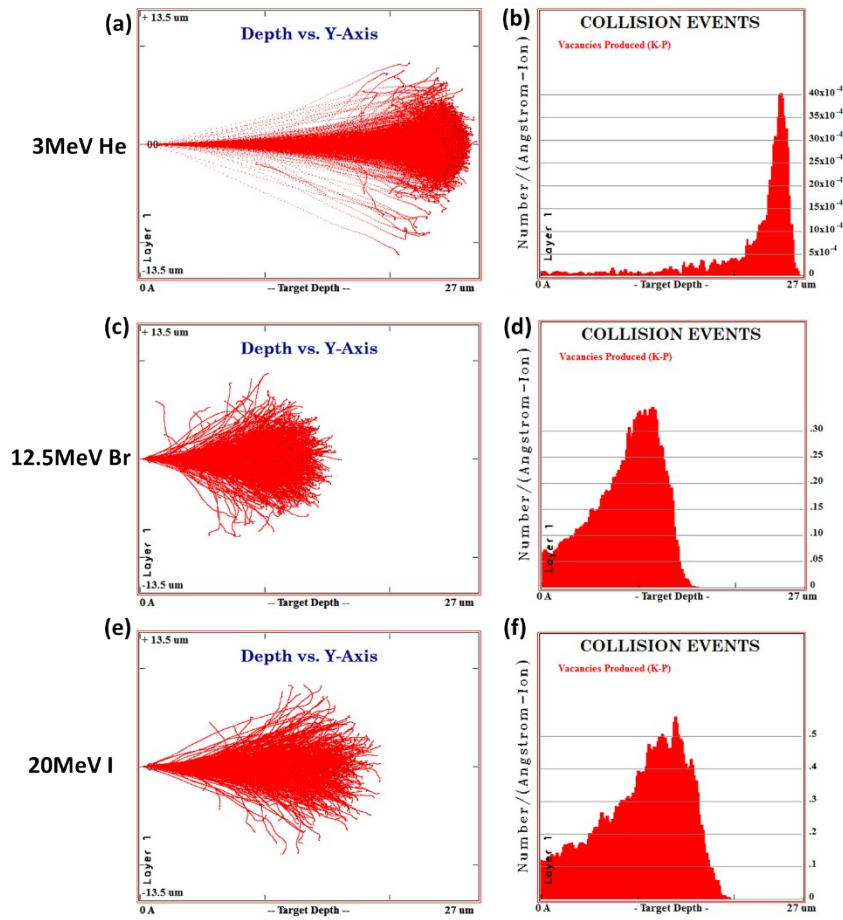


Fig. S5.1 The ion distribution and defect distribution in MAPbBr₃ calculated by SRIM³ for a, b) 3MeV He⁺, c, d) 12.5MeV Br⁵⁺, e, f) 20MeV I⁷⁺.

With the input of incident ion type, ion energy and target material, the vacancy number per Angstrom in depth per ion distribution along the depth is obtained, seen in Fig. S5.1. With its value at the surface (defined as D), the surface defect density (SDD) is calculated as $S^{DD} (vacancy/cm^3) = D \cdot ion\ dose \cdot 10^8$, where ion dose is in the unit of ion number/cm², and D is the vacancy number per Angstrom in depth per ion at the surface of MAPbBr₃. (Table S3)

Table S3. The ion type, ion dose, and calculated defect density at the surface of MAPbBr₃.

Ion type (mass)	Defect/Å/Ion at the surface	Dose (ions/cm ²)	Defect density at the surface (/cm ³)
He ⁺ (4)	0.0001	5×10 ¹¹	5×10 ¹⁵
		5×10 ¹²	5×10 ¹⁶
Br ⁵⁺ (79)	0.075	1×10 ¹¹	7.5×10 ¹⁷
		1×10 ¹²	7.5×10 ¹⁸
I ⁷⁺ (127)	0.15	1×10 ¹¹	1.5×10 ¹⁸
		1×10 ¹²	1.5×10 ¹⁹

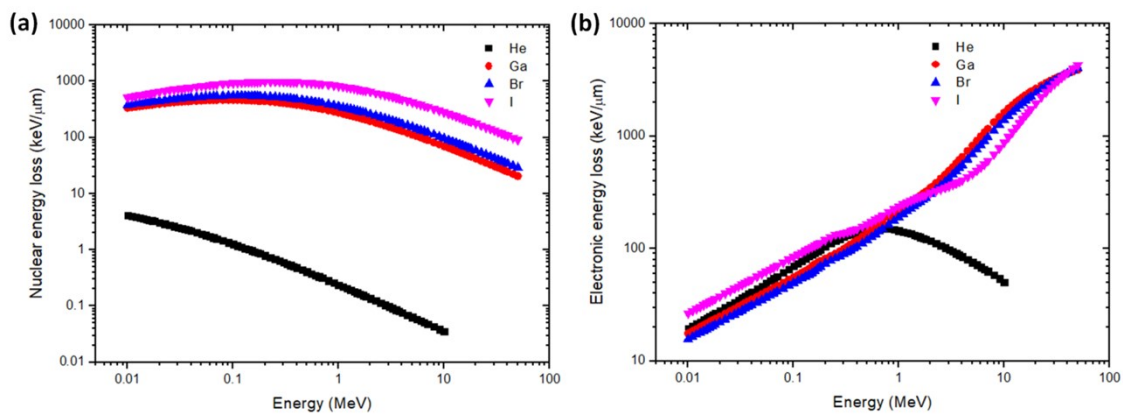


Fig. S5.2 The nuclear and electronic energy loss for He⁺, Br⁵⁺, I⁷⁺ in MAPbBr₃ calculated by SRIM³.

References:

1. M. A. Digman, V. R. Caiolfa, M. Zamaï and E. Gratton, *Biophysical Journal*, 2008, **94**, L14-L16.
2. J. R. Lakowicz, *Principles of fluorescence spectroscopy*, New York : Springer, 3rd ed.. edn., 2006.
3. J. F. Ziegler, M. D. Ziegler and J. P. Biersack, *Nucl. Instrum. Meth. B*, 2010, **268**, 1818-1823.